Society For Biomaterials

Subcutaneous tissue reaction and cytotoxicity of polyvinylidene fluoride and polyvinylidene fluoride-trifluoroethylene blends associated with natural polymers

Leonardo Marques,[1] Leandro A. Holgado,[1] Rebeca D. Simões,[2] João D. A. S. Pereira,[2] Juliana F. Floriano,[3] Lígia S. L. S. Mota,[4] Carlos F. O. Graeff,[3] Carlos J. L. Constantino,[2] Miguel. A. Rodriguez-Perez,[5] Mariza Matsumoto,[1] Angela Kinoshita[1]

[1]Universidade Sagrado Coração – USC, Bauru, São Paulo, Brazil
[2]Faculdade de Ciências e Tecnologia, UNESP Universidade Estadual Paulista, Presidente Prudente, São Paulo, Brazil
[3]Faculdade de Ciências, UNESP Universidade Estadual Paulista, Bauru, São Paulo, Brazil
[4]Instituto de Biociências, UNESP Universidade Estadual Paulista, Bauru, São Paulo, Brazil
[5]Condensed Matter Physics Department, CellMat Laboratory, Faculty of Science, University of Valladolid, Valladolid, Spain

Received 27 August 2012; revised 5 February 2013; accepted 6 March 2013
Published online 10 May 2013 in Wiley Online Library (wileyonlinelibrary.com). DOI: 10.1002/jbm.b.32941

Abstract: Cytotoxicity and subcutaneous tissue reaction of innovative blends composed by polyvinylidene fluoride and polyvinylidene fluoride-trifluoroethylene associated with natural polymers (natural rubber and native starch) forming membranes were evaluated, aiming its applications associated with bone regeneration. Cytotoxicity was evaluated in mouse fibroblasts culture cells (NIH3T3) using trypan blue staining. Tissue response was *in vivo* evaluated by subcutaneous implantation of materials in rats, taking into account the presence of necrosis and connective tissue capsule around implanted materials after 7, 14, 21, 28, 35, 60, and 100 days of surgery. The pattern of inflammation was evaluated by histomorphometry of the inflammatory cells. Chemical and morphological changes of implanted materials after 60 and 100 days were evaluated by Fourier transform infrared (FTIR) absorption spectroscopy and scanning electron microscopy (SEM) images. Cytotoxicity tests indicated a good tolerance of the cells to the biomaterial. The *in vivo* tissue response of all studied materials showed normal inflammatory pattern, characterized by a reduction of polymorphonuclear leukocytes and an increase in mononuclear leukocytes over the time ($p < 0.05$ Kruskal–Wallis). On day 60, microscopic analysis showed regression of the chronic inflammatory process around all materials. FTIR showed no changes in chemical composition of materials due to implantation, whereas SEM demonstrated the delivery of starch in the medium. Therefore, the results of the tests performed *in vitro* and *in vivo* show that the innovative blends can further be used as biomaterials. © 2013 Wiley Periodicals, Inc. J Biomed Mater Res Part B: Appl Biomater 101B: 1284–1293, 2013.

Key Words: biomaterial, piezoelectricity, tissue reaction, cytotoxicity, PVDF

How to cite this article: Marques L, Holgado LA, Simões RD, Pereira JDAS, Floriano JF, Mota LSLS, Graeff CFO, Constantino CJL, Rodriguez-Perez MA, Matsumoto M, Kinoshita A. 2013. Subcutaneous tissue reaction and cytotoxicity of polyvinylidene fluoride and polyvinylidene fluoride-trifluoroethylene blends associated with natural polymers. J Biomed Mater Res Part B 2013:101: 1284–1293.

INTRODUCTION

Currently the gold standard for the treatment of large bone defects is the autologous bone that stimulates a series of cellular and molecular events that result in repair of the recipient area. Autologous bone is obtained from various donor sites; however, the morbidity of this procedure, the technical difficulty, and the high costs are factors that make necessary the search for new biomaterials with properties that enhance bone healing.[1,2]

The most commonly used bioabsorbable polymers for bone tissue engineering are saturated aliphatic polymers such as poly(lactic acid) (PLA), poly(glycolic acid),[3] polycaprolactone (PCL), and their copolymer, among others. These based polymers and their derivatives have been successfully used as internal fracture fixation devices (orthopedic bioabsorbable osteofixation systems) for long bones in human, since the mid-1980.[4] Another polymeric systems used are starch-based blends. The starch is blended with thermoplastic polymers to increase their resistance against thermomechanical degradation and make them less brittle and more easily processed. Blends of starch with PCL and PLA have

Correspondence to: A. Kinoshita; e-mail: angela.kinoshita@usc.br
Contract grant sponsors: FAPESP (Fundação de Amparo à Pesquisa do Estado de São Paulo), CNPq (Conselho Nacional de Desenvolvimento Científico e Tecnológico), CAPES (Coordenação de Aperfeiçoamento de Pessoal de Nível Superior), FAP/USC (Fundação de Amparo à Pesquisa da Universidade Sagrado Coração)

been proposed as potential alternative biodegradable materials for a wide range of biomedical applications, including bone cements and bone substitutes.[5] The association of biosorbable polymers with therapeutic factors was also investigated. For instance, Hench and Paschall[6] studied the association of poly(D,L-lactic acid) (PLDLA) and bioactive glass to improve the osteoconductivity, guiding the bone growth as the glass degrades. Carsten et al.[7] developed composites with biodegradable polymers and carbonated calcium phosphate ($CaCO_3$). Macroporous were formed inside it due to fast degradation of PLDLA, promoting the bone formation, whereas the slowly degradable poly-L-lactide outside of composite ensures the mechanical stability. In contrast with the strategy of inserting a therapeutic factor in polymeric matrix, in the present work no therapeutic factors of bone tissue regeneration were added since the polymers used already presents a propriety that may induce bone growth.

Polyvinylidene fluoride (PVDF) and its copolymer polyvinylidene fluoride-trifluoroethylene P(VDF-TrFE) applied here present scientific and technological interest due to their ferro, pyro, and piezoelectric properties.[8,9] More recently, Hong et al.[10] developed nanograss structures of P(VDF-TrFE) and observed an enhancement of piezoelectricity. This property can be associated with bone growth induction, since bones are piezoelectric.[11–13] Callegari and Belangero evaluated the interface formed between P(VDF-TrFE) and PVDF tubes (piezoelectric and nonpiezoelectric) in rat bone tissue. The results of conventional optical microscopy and backscattered scanning electron microscopy (SEM) indicate that the piezoelectric effect has an important role in the new bone tissue formation inside the polymeric tubes.[14]

PVDF is formed by repeating units of $-CH_2-CF_2-$, corresponding to about 2000 monomeric units with an average length of about[8] 0.5 μm. Due to its electrical properties, literature reports a wide range of applications for this polymer, including optoelectronic, electromechanical and more recently, as a biomaterial.[15,18] PVDF is a biocompatible material and some applications include vascular suture[16,17]; mesh materials for abdominal hernia repair[18–20] as a substrate to enhance nerve fiber outgrowth[21]; controlled delivery of drugs[19]; tissue engineering and cell biology application including bone regeneration.[11,13] These applications are mainly due to the high piezoelectric activity of PVDF, which depends on its polar crystalline phase.

The β phase of PVDF, characterized by a zigzag conformation chain with planar orthorhombic crystal system and network parameters $a = 8.58$ Å, $b = 4.91$ Å, and $c = 2.56$ Å, presents the highest piezoelectric response. Thus it is the most desirable form[8]; however, the most common crystalline phase is the α phase (nonpolar). On the other hand, random copolymers of vinylidene fluoride (VDF) with trifluoroethylene (TrFE) when associated in an appropriated molar ratio of VDF and TrFE, crystallize directly into a polar ferroelectric phase, in a transplanar chain similar to the PVDF β phase, presenting pyroelectricity and piezoelectricity comparable to β PVDF, after passing by a poling process.[8]

Membranes of PVDF and P(VDF-TrFE) can be produced when associated with natural rubber (NR) and/or cornstarch. In a previous work, the fabrication procedure of these membranes was described.[22] This process of fabrication discards the necessity of organic solvents to dissolve the synthetic copolymer, contributing to biocompatibility. Besides, such processing enables the fabrication of membranes with suitable mechanical properties. These blends were previously characterized by Fourier transform infrared (FTIR) spectroscopy, SEM, X-ray diffraction, density, melt flow index, hardness, and thermal conductivity. The results showed that the polymers do not interact chemically with the additives leading to the formation of blends as physical mixtures where the additives are well dispersed within the blends at micrometer level. However, it was observed that the adhesion of the starch is better in the case of blends with P(VDF-TrFE).[23] Besides, the crystalline structures of the α-PVDF and ferroelectric P(VDF-TrFE) are preserved in the blends. The density, hardness, melt flow index, and thermal conductivity values of the blends are the ones expected from physical mixtures.[24]

Tests for development of a new biomaterial include several stages from *in vitro* tests through cell cultures and *in vivo* experiments using animal and human clinical trials. Such tests evaluate the biocompatibility, biological properties, and the risks that the material can cause to health.[12,24–27] Usually, the first stage to test a new material for biomedical use is the *in vitro* biocompatibility essays. In this work, the cytotoxicity of the polymeric blends was evaluated *in vitro* using the cell line NIH3T3 of mouse fibroblasts and *in vivo* by the study of tissue reaction after subcutaneous implant in rats. The results obtained with membranes prepared with P(VDF-TrFE) were compared to PVDF/starch/NR latex, that is composed by well-known biocompatible materials.[16,28–30] As already mentioned, PVDF and P(VDF-TrFE) present piezoelectricity and can contribute to bone growth, indicating that the blends studied in this work can be useful for procedures associated with bone regeneration. Besides, the presence of interconnected porous, generated by the presence of the starch in the blends, is another factor that contributes to the bone tissue growth.

MATERIALS AND METHODS

The present study was approved by the Ethical Committee from the Universidade Sagrado Coração – USC, Bauru, São Paulo State, Brazil and was conducted according to recommendations of the National Institute of Health.[31]

Membranes

The innovative blends in form of membranes of PVDF/starch/NR, P(VDF-TrFE)/starch and P(VDF-TrFE)/NR were prepared by compressing/annealing (2 tons at 180°C) powders of the starting material leading to membranes of 1 mm thick, as described in a previous work.[24] They were cut in circular shape with 5 mm diameter and sterilized with gamma radiation (25 kGy) for *in vivo* and *in vitro* studies. The PVDF used was Florafon F4000 HD acquired from Atochem and P(VDF-TrFE) was 72/28 (in mass) acquired from Piezotech (Piezotech S.A.S, Hésingue, France). The latex was collected from different trees of *Hevea brasiliensis*, clones

RRIM-600 (Rubber Research Institute of Malaysia), at the experimental farm of EMBRAPA in Indiana, Sao Paulo, Brazil. The latex stabilization was made by using a commercial solution of NH_4OH (4.7 mL of NH_4OH for 100 mL of latex). The regular cornstarch with 28% amylose and particle size of 10 μm (commercial name Amudex 3001) was supplied by Corn Products Brazil.

Cytotoxicity test

The biological properties of the materials were firstly evaluated by *in vitro* cell tests.[32] Cytotoxicity was evaluated by using the cell line NIH3T3 of mouse fibroblasts. The cells were placed in culture flasks (25 cm^2) with 3.0 mL of culture medium Dulbecco's modified Eagle's medium-HAM F12 (Invitrogen) 1:1 ratio, supplemented with 20% fetal bovine serum and 1% penicillin/streptomycin and incubated at 38°C with 95% humidity and 5% CO_2. When the cells reached their highest degree of proliferation, they were isolated by using trypsin (Trypsin-Versen solution; Institute Adolfo Lutz) for 3 min. The cell suspension obtained was transferred to a centrifuge tube for washing in culture media at 1000 rpm for 5 min. This procedure was repeated twice. In the end cells were suspended in 1 mL of culture medium.

The materials were placed in contact with the culture cells in concentration of 3.0×10^5 cells mL^{-1}, along with the culture medium and incubated in the same conditions previously described for a period of 72 h. After this period, the material was removed. All samples were tested in triplicate. The parameter used to evaluate toxicity was cell viability using Trypan blue staining as marker (Sigma-Aldrich Co.). Cell suspension of 40 μL was added to 40 μL of Trypan blue, homogeneized, and inoculated in a Neubauer chamber. Cell counting was performed in four quadrants of the external chamber. As negative control the culture plate itself was used and as positive control phenol (0.02%), to validate the test system. The stained blue cells were considered dead and the total viable cells was divided by the total number of quadrants (four) and multiplied by 20,000 (10,000 × dilution factor 2). The nonparametric test Kruskal–Wallis was used to compare the results and they were considered statistically different when $p < 0.05$.

The cell viability was observed only in the period of 72 h, following the period described in ISO 10993-5 and ASTM 19953, describing the periods of direct contact with the cells of the material by 72h.

Subcutaneous implant in vivo

A total of 27 male Wistar rats, weighing an average of 300 g, were used. The animals were kept in a plastic cage in an experimental animal room and were fed with standard laboratory diet and water. Preoperatively, general anesthetic was intramuscularly induced in animals with xylazine chlorhydrate (5 mg kg^{-1}; Bayer, Brazil) and ketamine (35 mg kg^{-1}; Vetbrands, Brazil). The dorsal part was shaved and aseptically prepared for surgery. Incisions of 1cm long were made along the back of the animal, symmetrical in relation to the midline, three on the right and three on the left side totalizing six incisions according to the model of Minnen et al.[33] The distance between implanted materials was approximately 3 cm.

The skin was separated exposing the subcutaneous tissue, where the membranes were implanted. Two samples of each blend were implanted into each animal in random position. The soft tissues and skin incisions were closed with 4-0 silk interrupted sutures. After 7, 14, 21, 28, and 35 days, three animals were euthanized, and the pieces containing the material removed microscopic and macroscopic analysis. Six samples ($n = 6$) for each material implanted for a period of observation were obtained. After 60 and 100 days, six animals were used: three for microscopic analysis and three for experiments to characterize the implanted material.

For microscopic analysis, the excised tissues were prepared following routine histology procedures, parafinized sections with 6 μm were stained with Masson's trichrome and hematoxilin and eosin. The photomicroscope Nikkon H550L was used to acquire the images. Six fields with 40× magnification around each implanted material were used for cell counting. Polymorphonuclear, mononuclear and giant cells (GCs) were counted and the thickness of fibrous connective tissue (CT) capsule was assessed using the software Image Pro-plus (Media-Cybernetics).

The average concentration of inflammatory cells in six fields was classified according to the distribution adapted from Yaltirik et al.[34]; for mononuclear and polymorphonuclear cells, the classification was (1) <50 cells; (2) 50–70 cells; (3) 70–100 cells, and (4) >100 cells and for GCs (1) <10 cells; (2) 10–20 cells, (3) 20–30 cells, and 4) >30 cells. This classification was adopted taking into account the distribution of values found. The nonparametric test Kruskal–Wallis was used to compare the results and they were considered statistically different when $p < 0.05$.

Characterization techniques of implanted membranes

The samples collected after 60 and 100 days postimplantation were accessed by FTIR, to examine the chemical changes of the blends and by SEM, to study their morphology. FTIR measurements were carried out with a Bruker spectrometer model Tensor 27 in the ATR mode (not polarized), using 64 scans, and 4 cm^{-1} spectral resolution. The SEM images were recorded using a JEOL microscope model JSM-820 (3 kV and 20 kV). The SEM were obtained from the transversal section after breaking the membranes through a fragile fracture (the membranes were frozen in liquid N_2), the Au metallization (ca. 20 nm) was carried out using a Balzers thermal evaporator model SCD 004.<

RESULTS

Macroscopic aspect postimplantation

Figure 1 shows the membranes in the region of implantation 60 days after surgery. The encapsulation of the implanted material can be seen as well as the normal aspect of the tissues adjacent to the materials.

Microscopic analysis

Figure 2 shows microscopic images of the implantation region of the membranes, in the initial and final periods

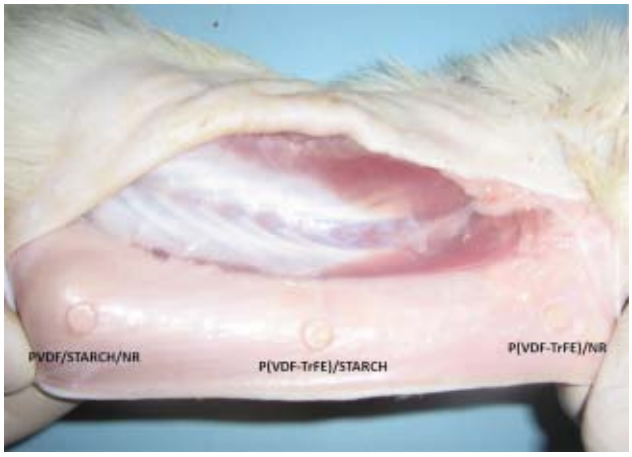

FIGURE 1. The membranes of PVDF/starch/NR, P(VDF-TrFE)/starch and P(VDF-TrFE)/NR 60 days after surgery. The normal aspect of the tissues adjacent to the materials can be observed. [Color figure can be viewed in the online issue, which is available at wileyonlinelibrary.com.]

after implantation. The region occupied by the membranes is marked (#). The images of 100 days after implantation suggest that the membranes remained unchanged. At higher magnification, see Figure 3, CT and inflammatory cells may be noted around the materials.

Tables I–III show the average counting of polymorphonuclear, mononuclear, and GCs after classification and are represented by the number of slices in the score divided by the total number of slices observed. The differences between the results were assessed by Kruskal–Wallis test and the same symbol inserted in superscript indicates $p < 0.05$. Table IV shows the average fibrous capsule thickness for each material as function of time. There are no statistically significant differences between periods or materials [$p > 0.05$ analysis of variance (ANOVA), Tukey].

The microscopic images demonstrate that all tested materials presented similar responses (Figs. 2 and 3). This result was statistically verified, since in general, there is no difference between the responses of materials in the same period. The statistically significant differences are found in the cell counting performed after implant of the same material in different periods (Table III).

Seven days after implant, the materials are surrounded by granulation tissue [CT; Fig. 3(a–c)], with a moderate number of mononuclear inflammatory cells infiltrate. Some parallel bundles of collagen fibers (*) can also be observed in the P(VDF-TrFE)/starch (b) and P(VDF-TrFE)/NR (c) images. At 14 days, organized CT with collagen fibers arranged parallel to each other in contact with materials are observed with a slight diffuse mononuclear inflammatory infiltrate. At 21 days, the microscopic pattern is similar to the previous period, with a decrease in the granulation tissue with persistence of mononuclear cell infiltration. In the PVDF/starch/NR results, the increase in mononuclear cells is statistically significant ($p < 0.05$) in comparison to the 7-day period (Table II) and the number of foreign body GCs associated with the implanted material is also in greater quantity ($p < 0.05$) in comparison to the 7-day period (Table III).

After 28 days, organization of collagen fibers with focal areas of mononuclear leukocytes is observed. In the P(VDF-TrFE)/starch images, vascular tissue close to the material is observed. An increase in the number of mononuclear cells and GCs in comparison to 7 days of implantation and a

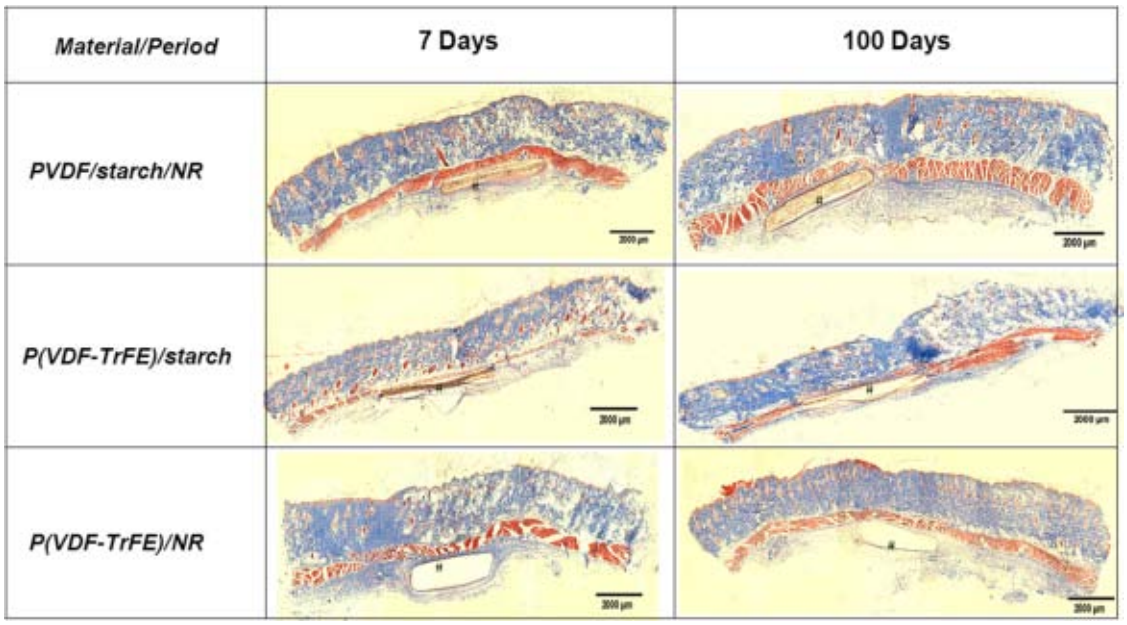

FIGURE 2. Microscopic images of the implantation region of the membranes, 7 and 100 days after surgery. The region occupied by the membranes is indicated (#). (Masson Trichrome staining, original magnification ×2). [Color figure can be viewed in the online issue, which is available at wileyonlinelibrary.com.]

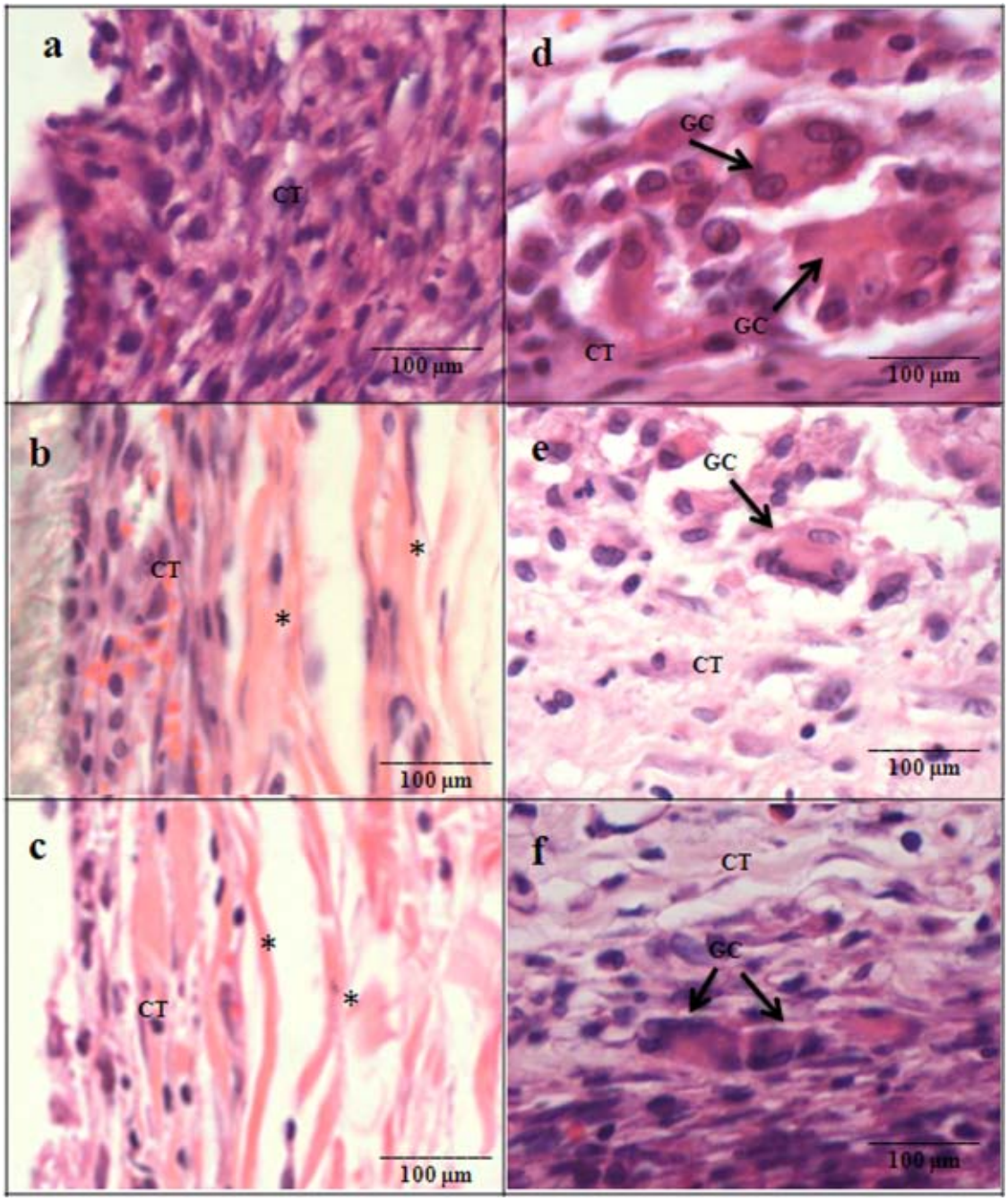

FIGURE 3. Microscopic images of the implantation region of the membranes, 7 (a–c) and 100 days (d–f) after surgery at higher magnification of P(VDF-TrFE) (a and d), P(VDF-TrFE)/starch (b and e), and P(VDF-TrFE)/NR (c and f). At 7 days a moderate mononuclear inflammatory infiltrate in the connective tissue (CT) is present. Parallel bundles of collagen fibers (*) surrounding the material are also observed. At 100 days, multinucleated giant cells (GCs) in association with the membrane (hematoxylin and eosin staining, original magnification ×40). [Color figure can be viewed in the online issue, which is available at wileyonlinelibrary.com.]

significant reduction in polymorphonuclear cells are found ($p < 0.05$, Tables I) in the P(VDF-TrFE)/starch and P(VDF-TrFE)/NR cell counting.

After 35 days, all tested implanted materials presented surrounded by mature fibrous CT showing collagen fibers parallel to each other, with a capsular pattern. There is a reduction in the number of polymorphonuclear cells, increase in mononuclear and GCs, in comparison with the beginning period ($p < 0.05$; Tables I).

After 60 days of implantation, a reduction in the inflammation pattern is noticed for all tested materials, with a reduction in polymorphonuclear cells and an increase in the number of mononuclear and GCs in comparison with the initial periods ($p < 0.05$, Tables I). Similar results are

TABLE I. Results of Classification of the Average of Polymorphonuclear Cells According to the Material and Period of Implant

Period (Days)	Material	1	2	3	4
7	PVDF/starchNR^{abc}	0/6	1/6	5/6	0/6
	P(VDF-TrFe)/starch^{ij}	0/6	4/6	2/6	0/6
	P(VDF-TrFe)/NR^{rstuv}	0/6	0/6	6/6	0/6
14	PVDF/starch/NR^{def}	0/6	2/6	4/6	0/6
	P(VDF-TrFe)/starch^{kl}	0/6	4/6	2/6	0/6
	P(VDF-TrFe)/NR^{vxyz}	0/6	0/6	6/6	0/6
21	PVDF/starch/NR^{gh}	0/6	6/6	0/6	0/6
	P(VDF-TrFe)/starch^{mno}	0/6	5/6	1/6	0/6
	P(VDF-TrFe)/NR$^{w*\#}$	0/6	4/6	2/6	0/6
28	PVDF/starch/NR	1/6	5/6	0/6	0/6
	P(VDF-TrFe)/starch^{pq}	0/6	5/6	1/6	0/6
	P(VDF-TrFe)/NR^{rv}	2/6	4/6	0/6	0/6
35	PVDF/starch/NR^{ad}	5/6	1/6	0/6	0/6
	P(VDF-TrFe)/starch^{m}	2/6	4/6	0/6	0/6
	P(VDF-TrFe)/NR^{sxw}	5/6	1/6	0/6	0/6
60	PVDF/starch/NR^{beg}	6/6	0/6	0/6	0/6
	P(VDF-TrFe)/starch^{iknp}	6/6	0/6	0/6	0/6
	P(VDF-TrFe)/NR^{ty*}	6/6	0/6	0/6	0/6
100	PVDF/starch/NR^{cfh}	6/6	0/6	0/6	0/6
	P(VDF-TrFe)/starch^{jloq}	6/6	0/6	0/6	0/6
	P(VDF-TrFe)/NR$^{uz\#}$	6/6	0/6	0/6	0/6

a–z, *#: the same symbol indicates differences statistically significant, $p < 0.05$ (Kruskal–Wallis followed by Student–Newman–Keuls).

observed at 100-day period with the same statistical pattern found at 60 days, certifying the normal microscopic feature of the underlying tissues of the implant. Multinucleated GCs in association with the materials are observed [Fig. 3(d–f)].

TABLE II. Results of the Classification of the Average of Mononuclear Cells According to the Material and Period of Implant

Period (Days)	Material	1	2	3	4
7	PVDF/starch/NR^{abcd}	0/6	4/6	2/6	0/6
	P(VDF-TrFe)/starch^{ijkl}	2/6	4/6	0/6	0/6
	P(VDF-TrFe)/NR^{mnop}	3/6	3/6	0/6	0/6
14	PVDF/starch/NR^{efgh}	0/6	4/6	2/6	0/6
	P(VDF-TrFe)/starch	0/6	4/6	2/6	0/6
	P(VDF-TrFe)/NR^{qrs}	2/6	4/6	0/6	0/6
21	PVDF/starch/NR$^{ae\#}$	0/6	0/6	6/6	0/6
	P(VDF-TrFe)/starch	0/6	3/6	3/6	0/6
	P(VDF-TrFe)/NR$^{tu\#}$	0/6	6/6	0/6	0/6
28	PVDF/starch/NR	0/6	2/6	4/6	0/6
	P(VDF-TrFe)/starch^{i}	0/6	1/6	5/6	0/6
	P(VDF-TrFe)/NR^{m}	0/6	3/6	3/6	0/6
35	PVDF/starch/NR^{bf}	0/6	0/6	6/6	0/6
	P(VDF-TrFe)/starch^{j}	0/6	0/6	6/6	0/6
	P(VDF-TrFe)/NR^{nq}	0/6	2/6	4/6	0/6
60	PVDF/starch/NR^{cg}	0/6	0/6	6/6	0/6
	P(VDF-TrFe)/starch^{k}	0/6	0/6	6/6	0/6
	P(VDF-TrFe)/NR^{ort}	0/6	0/6	6/6	0/6
100	PVDF/starch/NR^{dh}	0/6	0/6	6/6	0/6
	P(VDF-TrFe)/starch^{l}	0/6	0/6	6/6	0/6
	P(VDF-TrFe)/NR^{psu}	0/6	0/6	3/6	3/6

a–u: The same symbol indicates differences statistically significant, $p < 0.05$ (Kruskal–Wallis followed by Student–Newman–Keuls).

TABLE III. Results of the Classification of the Average of Giant Cells According to the Material and Period of Implant

Period (Days)	Material	1	2	3	4
7	PVDF/starch/NR^{abcd}	4/6	2/6	0/6	*0/6*
	P(VDF-TrFe)/starch^{jkl}	4/6	2/6	0/6	*0/6*
	P(VDF-TrFe)/NR^{uvxy}	6/6	0/6	0/6	*0/6*
14	PVDF/starch/NR^{efghi}	6/6	0/6	0/6	*0/6*
	P(VDF-TrFe)/starch^{mno}	6/6	0/6	0/6	*0/6*
	P(VDF-TrFe)/NR$^{zw*@}$	6/6	0/6	0/6	*0/6*
21	PVDF/starch/NR$^{\#ae}$	0/6	4/6	0/6	*2/6*
	P(VDF-TrFe)/starch$^{\#pqr}$	6/6	0/6	0/6	*0/6*
	P(VDF-TrFe)/NR$^{\%\$}$	2/6	4/6	0/6	*0/6*
28	PVDF/starch/NR^{*bf}	0/6	1/6	4/6	*1/6*
	P(VDF-TrFe)/starch^{*st}	2/6	3/6	1/6	*0/6*
	P(VDF-TrFe)/NR^{uz}	0/6	5/6	1/6	*0/6*
35	PVDF/starch/NR^{cg}	0/6	0/6	3/6	*3/6*
	P(VDF-TrFe)/starch^{jmps}	0/6	0/6	4/6	*4/6*
	P(VDF-TrFe)/NR$^{vw\%}$	0/6	1/6	456	*0/6*
60	PVDF/starch/NR^{h}	0/6	4/6	2/6	*0/6*
	P(VDF-TrFe)/starch^{kq}	0/6	1/6	5/6	*0/6*
	P(VDF-TrFe)/NR^{x*}	0/6	2/6	4/6	*0/6*
100	PVDF/starch/NR^{di}	0/6	1/6	3/6	*2/6*
	P(VDF-TrFe)/starch^{lort}	0/6	0/6	4/6	*2/6*
	P(VDF-TrFe)/NR$^{v@\$}$	*0/6*	*2/6*	*3/6*	*1/6*

a–z, *@, #, %, $, and @: The same symbol indicates differences statistically significant, $p < 0.05$ (Kruskal–Wallis followed by Student–Newman–Keuls).

FTIR and SEM results

Figure 4 shows FTIR measurements of P(VDF-TrFE)/starch, P(VDF-TrFE)/NR and PVDF/starch/NR membranes before and 60 and 100 days after implantation. The FTIR spectra of starch, NR, PVDF, and P(VDF-TrFE) are also presented.

Figure 5(a–f) shows the SEM images for membranes (a) before, (b) after 60-day implantation, and (c) 100-day implantation.

Cytotoxicity results

For all materials used, a low number of dead cells is observed compared to the positive control (0.02% phenol). The level of cell death observed was very similar to the negative control (culture plate). Cell viability of PVDF/starch/NR, P(VDF-TrFE)/starch, P(VDF-TrFE)/NR, and negative control were 82.9%, 86.5%, 89.2%, and 89.4%, respectively. There are no statistically significant differences among these results ($p > 0.05$ Kruskal–Wallis).

TABLE IV. Results of the Average and Standard Deviation of Thickness of Connective Tissue Capsule According to the Material and Period

Period (Days)	PVDF/ Starch/ NR (μm)	P(VDF-TrFe)/ Starch (μm)	P(VDF-TrFe)/ NR (μm)
35	50 ± 20	50 ± 20	50 ± 10
60	50 ± 10	45 ± 8	47 ± 9
100	50 ± 10	42 ± 5	46 ± 6

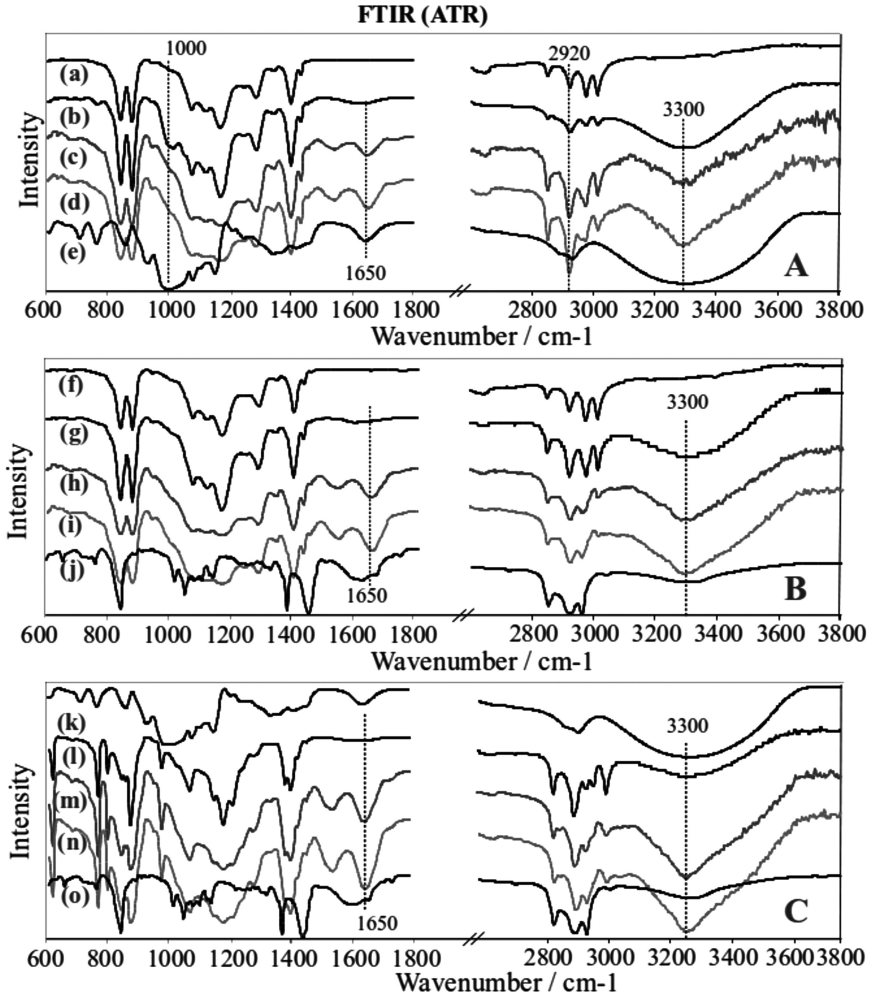

FIGURE 4. A: FTIR spectra of membranes of (a) P(VDF-TrFE) and (b) P(VDF-TrFE)/starch (before implantation). P(VDF-TrFE)/starch after implantation for (c) 60 days and (d) 100 days. (e) Starch powder. B: FTIR spectra of membranes of (f) P(VDF-TrFE) and (g) P(VDF-TrFE)/NR (before implantation). P(VDF-TrFE)/NR after implantation for (h) 60 days and (i) 100 days; (j) NR film. (C) FTIR spectra for starch powder (k) and (l) PVDF/starch/NR film (before implantation). PVDF/starch/NR film after implantation for (m) 60 days and (n) 100 days. o: NR film.

DISCUSSION

Fukada and Yasuda[35] demonstrated that bone is piezoelectric. Mechanical stress results in electric polarization and an applied electric field causes strain, the converse effect. It is assumed that the surface of bone in remodeling is governed, at least in part, by the piezoelectric polarization produced when the bone is deformed.[36] So, the association between piezoelectric materials and natural polymers with biological activity results in a promising material for bone repair. Marino et al.[11] implanted piezoelectric and nonpiezoelectric PVDF in rats and verified higher bone formation with piezoelectric PVDF, showing that materials with electrical polarization can alter bone cell function. In the same way, Gimenes et al.[13] showed that the piezoelectricity produced by membranes made of P(VDF-TrFE) associated with barium titanate induce bone regeneration in rabbit tibiae, demonstrating the relationship between biological mechanisms and electrical phenomena in the osteogenesis. The *in vitro* biocompatibility and the biological mechanisms associated with bone formation were also investigated using osteoblastic cells from human alveolar bone[37,38] and using human periodontal ligament fibroblasts.[39] NR is a biocompatible material[28] and some studies showed its potential in angiogenesis,[40] thus the association with piezoelectric materials might be interesting as a biomaterial for bone defect treatment.

Literature reports that cytotoxicity experiments are suitable initial test recommended to evaluate new materials.[41] The cell viability of all samples and negative control was the same ($p > 0.05$, Kruskal–Wallis) and higher than 50%. For this reason, all materials can be considered biocompatible.

Since *in vitro* results are more limited in scope than *in vivo*, in this work *in vivo* experiments were also used to evaluation of biological responses. For that purpose materials were implanted in the subcutaneous tissue of small animals. This method is considered one of the most appropriate for this application.[42–44] In this work the animal model and periods of observation were adopted following ISO-10993.[25,26] The macroscopic analysis of all pieces collected in postimplantation revealed that all the different

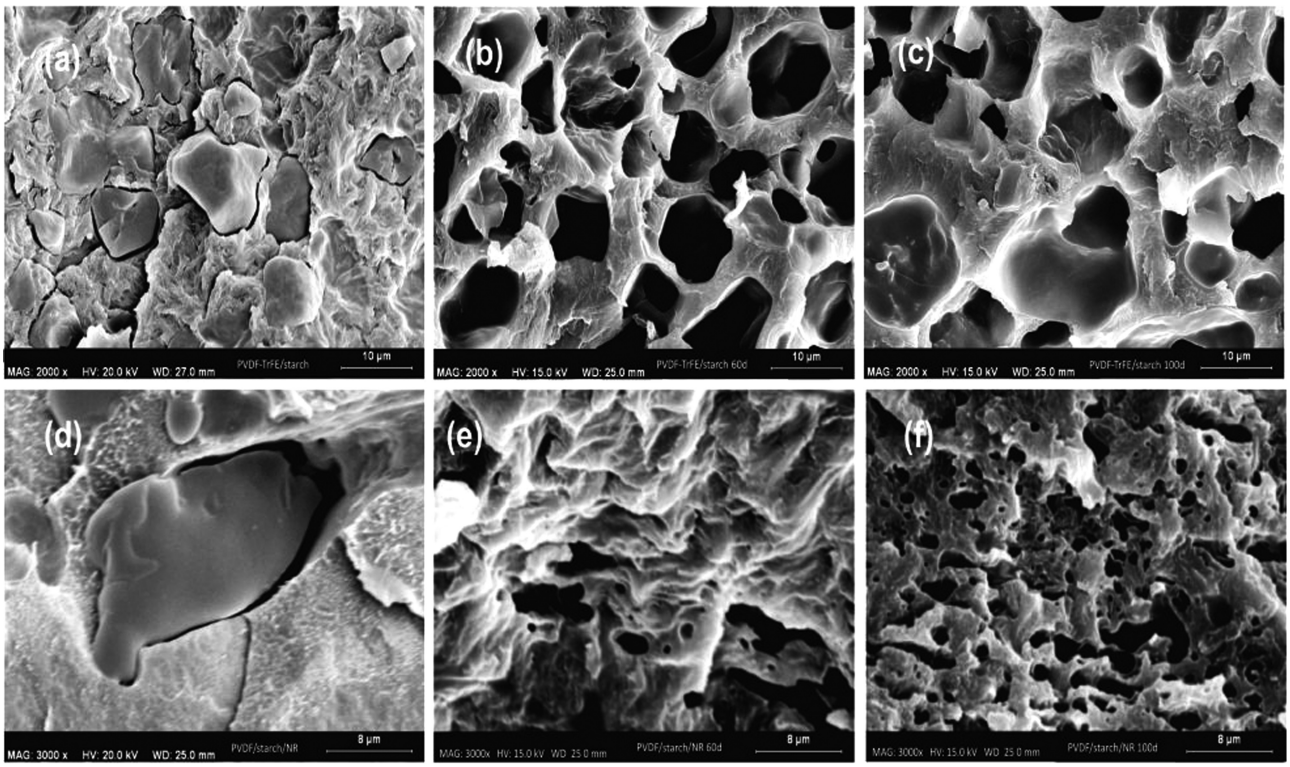

FIGURE 5. SEM for films of P(VDF-TrFE)/starch nonimplanted (a) and postimplanted with periods of (b) 60 days and (c) 100 days (cross-section). SEM for films of PVDF/starch/NR nonimplanted (d) and postimplanted with periods of (e) 60 days and (f) 100 days (cross-section).

materials used remained intact without any signs of degradation. The tissues adjacent to the implanted material presented normal characteristics, with no sign of rejection or severe inflammatory response. The microscopic analysis revealed in all cases that there is an inflammatory reaction in the initial periods, followed by chronic inflammatory features that evolve during tissue regeneration. The counting of inflammatory cells (Tables I) showed a normal inflammatory process, characterized by reduction of polimorphonuclear cells and increase in mononuclear and GCs over time, for all studied materials ($p < 0.05$, Kruskal–Wallis). The presence of polymorphonuclear cells in larger quantities particularly observed in earlier periods (7 and 14 days) in all tested materials is expected in the initial processes of inflammation after an acute tissue aggression.[45] In every stage analyzed, there are no statistically significant differences in the number of inflammatory cells among the materials studied. Fibrous capsule is present around all materials after 35 days postimplantation (Fig. 2; Table IV), and there are no differences in their thickness over time ($p > 0.05$ ANOVA).

Figure 4 show FTIR measurements of (A) P(VDF-TrFE)/-starch, (B) P(VDF-TrFE)/NR, and (C) PVDF/starch/NR membranes before and 60 and 100 days after implantation. The main assignments of the FTIR bands for native corn starch are based on literature.[46,47] The FTIR spectra of the polymers (PVDF and its copolymer) in postimplanted membranes are similar to those in nonimplanted membranes, which indicate the polymer (matrix) does not present chemical changes in their molecular structures for the implanted period of 60 and 100 days. However, some differences were found due to the action of the body on the starch in the implanted membranes. For instance, for P(VDF-TrFE)/starch, the band at 1000 cm^{-1} (C–O stretching), which is dominant in the spectrum of neat starch [Fig. 4(e)] and is present in the membrane before implantation [Fig. 4(b)], is hardly seen in the postimplanted membranes [Fig. 4(c,d)]. The same behavior was observed for the band at 3300 cm^{-1} (O–H stretching), which is strong in the spectra of neat starch [Fig. 4(e)] and in the membrane before implantation [Fig. 4(b)], but has its relative intensity decreased in comparison to the band at 2920 cm^{-1} (C–H stretching) for the postimplanted membranes [Fig. 4(c,d)]. These results suggest the absorption of starch by the animal.

On the other hand, the band attributed to water at 1650 cm^{-1} (O–H scissoring) has a different behavior. It appears in neat starch [Fig. 4(e,k)], but its relative intensity decreases in the nonimplanted membranes and increases in postimplanted membranes for all samples (A–C). This result is understood since the nonimplanted membranes are made at 180°C; therefore, they have less moisture. The implanted membranes remain in contact with body fluids and thus water is incorporated, despite the fact that starch is absorbed. In case of P(VDF-TrFE)/NR, particularly, the only differences between the FTIR spectra of the membranes before and after implantation are in the bands related to water adsorption (1650 and 3300 cm^{-1}). In relation to NR,

no change was identified. It is worth mentioning that the band at 3300 cm^{-1}, assigned to O–H stretching, can be related to water and starch content. Therefore, its relative intensity tends to increase with water adsorption within the postimplanted membranes and decrease with starch absorption by the body.

SEM images were obtained from cross-section (cryogenic fracture) for the membranes of P(VDF-TrFE)/starch and PVDF/starch/NR. Figure 5(a–f) shows the SEM images for membranes (a, d) before, (b, e) after 60-day implantation and (c, f) 100-day implantation. Pores are clearly seen in the implanted membranes, which is consistent with starch absorption suggested by FTIR. For PVDF/starch/NR membranes, it seems to be an increase in the number of pores with implantation time, which indicates that NR may hinder starch absorption.

CONCLUSION

The blends tested in this work, PVDF and P(VDF-TrFE) associated with natural polymers (NR and native starch) forming membranes do not present cytotoxicity from *in vitro* results. The tissue response after implantation presents reduction in inflammatory response with concomitant material encapsulation, a reduction in the number of polymorphonuclear cells and increase in mononuclear and GCs over time. The membranes with starch in its composition lose starch with implantation time (starch is absorbed by the body), leading to formation of interconnected porous, which may also contribute to bone tissue growth. Besides, the polymeric matrix (PVDF and P(VDF-TrFE)) does not present chemical changes even after 100 days after implantation. Therefore, our results attest favorable tissue reaction to these innovative blends for bone regeneration.

ACKNOWLEDGMENTS

The authors are grateful to Prof. Dr. A.E. Job from UNESP/Brazil and Prof. Dr. A.J.F. Carvalho from UFSCar/Brazil for supplying the latex and the cornstarch, respectively.

REFERENCES

1. Banwart JC, Asher MA, Hassanein RS. Iliac crest bone graft harvest donor site morbidity: A statistical evaluation. Spine 1995;20(9):1055–1060.
2. Bloemers FW, Blokhuis TJ, Patka P, Bakker FC, Wippermann BW, Haarman HJTM. Autologous bone versus calcium–phosphate ceramics in treatment of experimental bone defects. J Biomed Mater Res Part B: Appl Biomater 2003;66B(2):526–531.
3. Muhammad IS, Xiaoxue X, Li L. A review on biodegradable polymeric materials for bone tissue engineering applications. J Mater Sci 2009;44(21):5713–5724.
4. Warren SM, Fong K, Nacamuli RP, Fang TD, Longaker MT. Biomaterials for skin and bone replacement and repair in plastic surgery. Operat Tech Plast Reconstr Surg 2003;9(1):10–15.
5. Puppi D, Chiellini F, Piras AM, Chiellini E. Polymeric materials for bone and cartilage repair. Prog Polym Sci 2010;35(4):403–440.
6. Hench LL, Paschall HA. Direct chemical bond of bioactive glass–ceramic materials to bone and muscle. J Biomed Mater Res 1973;7(3): 35–42.
7. Carsten S, Christian R, Michael W, Felix B, Harald E, Matthias E, Stephan W. Geometrically structured implants for cranial reconstruction made of biodegradable polyesters and calcium phosphate/calcium carbonate. Biomaterials 2004;25(7):1239–1247.
8. Nalwa HS. Ferroelectric Polymers: Chemistry, Physics and Applications. New York: Marcel Dekker; 1995.
9. Fukada E, Furukawa T. Piezoelectricity and ferroelectricity in polyvinylidene fluoride. Ultrasonics 1981;19(1):31–39.
10. Hong C-C, Huang S-Y, Shieh J, Chen S-H. Enhanced piezoelectricity of nanoimprinted sub-20 nm poly(vinylidene fluoride–trifluoroethylene) copolymer nanograss. Macromolecules 2012;45(3):1580–1586.
11. Marino AA, Rosson J, Gonzalez E, Jones L, Rogers S, Fukada E. Quasi-static charge interactions in bone. J Electrostat 1988;21 (2–3):347–360.
12. Peppas NA, Langer R. New challenges in biomaterials. Science 1994;263:1715–1720.
13. Gimenes R, Zaghete MA, Bertolini MJ, Varela JA, Coelho LO, Silva NF Jr. Composites PVDF-TrFE/BT used as bioactive membranes for enhancing bone regeneration. Proc SPIE 2004;5385: 539–547.
14. Callegari B, Belangero WD. Analysis of the interface formed among the poly(vinylidene) fluoride (piezoelectric and non-piezoelectric) and the bone tissue of rats. Acta Ortop Bras 2004;12(3): 160–166.
15. Lang SB, Muensit S. Review of some lesser-known applications of piezoelectric and pyroelectric polymers. Appl Phys A: Mater Sci Process 2006;85(2):125–134.
16. Laroche G, Marois Y, Schwarz E, Guidoin R, King MW, Pâris E, Douville Y. Polyvinylidene fluoride monofilament sutures: Can they be used safely for long-term anastomoses in the thoracic aorta? Artif Organs 1995;19(11):1190–1199.
17. Bouaziz A, Richert A, Caprani A. Vascular endothelial cell responses to different electrically charged poly(vinylidene fluoride) supports under static and oscillating flow conditions. Biomaterials 1997;18(2):107–112.
18. Klinge U, Klosterhalfen B, Öttinger AP, Junge K, Schumpelick V. PVDF as a new polymer for the construction of surgical meshes. Biomaterials 2002;23(16):3487–3493.
19. Junge K, Rosch R, Klinge U, Krones C, Klosterhalfen B, Mertens PR, Lynen P, Kunz D, Preiß A, Peltroche-Llacsahuanga H, Schumpelick V. Gentamicin supplementation of polyvinyl fluoride mesh materials for infection prophylaxis. Biomaterials 2005;26(7):787–793.
20. Conze J, Junge K, Weiß C, Anurov M, Oettinger A, Klinge U, Schumpelick V. New polymer for intra-abdominal meshes—PVDF copolymer. J Biomed Mater Res Part B: Appl Biomater 2008;87B (2):321–328.
21. Lee Y-S, Collins G, Livingston Arinzeh T. Neurite extension of primary neurons on electrospun piezoelectric scaffolds. Acta Biomater 2011;7(11):3877–3886.
22. Simoes RD, Job AE, Chinaglia DL, Zucolotto V, Camargo-Filho JC, Alves N, Giacometti JA, Oliveira ON, Constantino CJL. Structural characterization of blends containing both PVDF and natural rubber latex. J Raman Spectro 2005;36(12):1118–1124.
23. Simoes R, Rodriguez-Perez M, de Saja J, Constantino C. Thermomechanical characterization of PVDF and P(VDF-TrFE) blends containing cornstarch and natural rubber. J Therm Anal Calorim 2010;99(2):621–629.
24. Simoes RD, Rodriguez-Perez MA, De Saja JA, Constantino CJL. Tailoring the structural properties of PVDF and P(VDF-TrFE) by using natural polymers as additives. Polym Eng Sci 2009;49(11): 2150–2157.
25. ISO 10993-1:2009. Biological evaluation of medical devices. Part 1: Evaluation and testing in the risk management process.
26. ISO 10993-2:2006. Biological evaluation of medical devices. Part 2: Animal welfare requirements.
27. Wataha JC. Predicting clinical biological responses to dental materials. Dent Mater 2012;28(1):23–40.
28. Balabanian CACA, Coutinho-Netto J, Lamano-Carvalho TL, Lacerda SA, Brentegani LG. Biocompatibility of natural latex implanted into dental alveolus of rats. J Oral Sci 2006;48(4):201–205.
29. Chunyan L, Pei-Ming W, Soohyun L, Gorton A, Schulz MJ, Ahn CH. Flexible dome and bump shape piezoelectric tactile sensors using PVDF-TrFE copolymer. J Microelectromech Syst 2008; 17(2):334–341.

30. Klink CD, Junge K, Binnebosel M, Alizai HP, Otto J, Neumann UP, Klinge U. Comparison of long-term biocompatibility of PVDF and PP meshes. J Investig Surg 2011;24(6):292–299.
31. Janet, CG, Barbee, RW, Bielitzki, JT, Clayton, LA, Donovan, JC, Hendriksen, CFM, Kohn, DF, Lipman, NS, Locke, PA, Melcher, J, Quimby, FW, Turner, PV, Wood, GA, Würbel, H. Guide for the Care and Use of Laboratory Animals, 8th ed, Washington, DC: National Academies Press; 2011.
32. Strober W. Trypan blue exclusion test of cell viability. In: Coligan JE, editor. Current Protocols in Immunology. New York: Wiley & Sons; 2003.
33. Minnen B, Leeuwen M, Stegenga B, Zuidema J, Hissink C, Kooten T, Bos R. Short-term in vitro and in vivo biocompatibility of a biodegradable polyurethane foam based on 1,4-butanediisocyanate. J Mater Sci: Mater Med 2005;16(3):221–227.
34. Yaltirik M, Ozbas H, Bilgic B, Issever H. Reactions of connective tissue to mineral trioxide aggregate and amalgam. J Endod 2004;30(2):95–99.
35. Fukada E, Yasuda I. On the piezoelectric effect of bone. J Phys Soc Jpn 1957;12(10):1158–1162.
36. A G. Bone remodeling and piezoelectricity—I. J Biomech 1973;6(1):69–77.
37. Beloti MM, de Oliveira PT, Gimenes R, Zaghete MA, Bertolini MJ, Rosa AL. In vitro biocompatibility of a novel membrane of the composite poly(vinylidene-trifluoroethylene)/barium titanate. J Biomed Mater Res Part A 2006;79A(2):282–288.
38. Teixeira L, Crippa G, Gimenes R, Zaghete M, de Oliveira P, Rosa A, Beloti M. Response of human alveolar bone-derived cells to a novel poly(vinylidene fluoride-trifluoroethylene)/barium titanate membrane. J Mater Sci: Mater Med 2011;22(1):151–158.
39. Teixeira LN, Crippa GE, Trabuco AC, Gimenes R, Zaghete MA, Palioto DB, de Oliveira PT, Rosa AL, Beloti MM. In vitro biocompatibility of poly(vinylidene fluoride–trifluoroethylene)/barium titanate composite using cultures of human periodontal ligament fibroblasts and keratinocytes. Acta Biomater 2010;6(3):979–989.
40. Mendonça RJ, Maurício VB, de Bortolli Teixeira L, Lachat JJ, Coutinho-Netto J. Increased vascular permeability, angiogenesis and wound healing induced by the serum of natural latex of the rubber tree *Hevea brasiliensis*. Phytother Res 2010;24(5):764–768.
41. Cao T, Saw TY, Heng BC, Liu H, Yap AUJ, Ng ML. Comparison of different test models for the assessment of cytotoxicity of composite resins. J Appl Toxicol 2005;25(2):101–108.
42. Olsson B, Sliwkowski A, Langeland K. Subcutaneous implantation for the biological evaluation of endodontic materials. J Endod 1981;7(8):355–369.
43. Safavi KE, Pascon EA, Langeland K. Evaluation of tissue reaction to endodontic materials. J Endod 1983;9(10):421–429.
44. Dawlee S and Jayabalan M. Iodinated glycidyl methacrylate copolymer as a radiopaque material for biomedical applications. J Biomater Appl. DOI: 10.1177/0885328211434090.
45. Parirokh M, Mirsoltani B, Raoof M, Tabrizchi H, Haghdoost AA. Comparative study of subcutaneous tissue responses to a novel root-end filling material and white and grey mineral trioxide aggregate. Int Endod J 2011;44(4):283–289.
46. Mano JF, Reis RL. Viscoelastic monitoring of starch-based biomaterials in simulated physiological conditions. Mater Sci Eng A 2004;370(1–2):321–325.
47. Park JW, Im SS, Kim SH, Kim YH. Biodegradable polymer blends of poly(L-lactic acid) and gelatinized starch. Polym Eng Sci 2000;40(12):2539–2550.